CHAPTER VI

COMPARATIVE STUDY ON INFLUENCE OF SECOND METALS ON Ag-LOADED MESOPOROUS $SrTiO_3$ CATALYSTS FOR ETHYLENE OXIDE EVOLUTION

(Submitted to Journal of Molecular Catalysis A: Chemical)

6.1 Abstract

Ag/Mesoporous-assembled $SrTiO_3$ catalysts with different loaded second metals (Au, Ba, Pd, Sn, and Cu) were tested for the catalytic activity towards ethylene oxide formation from the epoxidation reaction of ethylene, in comparisons to Ag- and Au-loaded on the $SrTiO_3$ supports. To promote long-term stability, Sn was added to the optimum bimetallic catalyst. The catalysts were analytically characterized by Brunauer–Emmett–Teller (BET) surface area, X-ray diffraction (XRD), field emission scanning electron microscopy (FE-SEM), transmission electron microscopy (TEM), energy-dispersive X-ray spectroscopy (EDS), temperature programmed desorption (TPD), and X-ray photoelectron spectroscopy (XPS) analyses. The addition of a second metal of Au, Ba, or Cu significantly improved the catalytic performance for ethylene epoxidation, whereas the Pd and Sn did not. The Cu-Ag bimetallic catalyst exhibited the highest catalytic ethylene oxide production activity. Moreover, an addition of Sn to this catalyst greatly promoted the long-term stability towards the ethylene epoxidation.

Keywords: Ethylene oxide; $SrTiO_3$; Silver catalyst; Bimetallic catalyst; Cu-Ag

6.2 Introduction

Silver is one of active heterogeneous catalysts to be used for a number of industrially important chemical reactions, including ethylene epoxidation. The epoxidation of ethylene to ethylene oxide (EO) is generally carried out over silver catalysts on low-surface-area alumina support at a reaction temperature in the range of 500-600 K under atmospheric pressure [1-2]. CO_2 is the main undesirable non-selective product formed from the burning of both ethylene and EO. The formation of CO_2 is highly exothermic and so the ethylene conversion has to be maintained at a low temperature under O_2 lean condition in order to control excess heat released by the complete combustion reaction, resulting in lowering undesired CO_2 end product [3-4]. As a consequence, the ethylene conversion is very low in the range of 10-15 % with less than 10 % being more typical, while a maximum EO selectivity is typically about 85-90 % [5]. The selectivity towards this reaction was found to increase with increasing oxygen coverage [6]. It has been reported that ethylene oxide formation is governed by adsorbed oxygen in two states: 'ionic' (nucleophilic) oxygen which is similar to that in Ag_2O (the lowly active oxide, easily forming on small Ag particles which decreases the epoxidation rate) and 'covalent' (electrophilic) oxygen localized at the surface defects. The nucleophilic oxygen (or Ag^+ cations involved) serves for the ethylene adsorption, while the electrophilic oxygen reacts with the C_2H_4 molecule, yielding EO. Thus, the pair of both oxygen types is required. In the presence of nucleophilic oxygen alone, the adsorbed ethylene subsequently reacts to form the products of deep oxidation only [7]. It was shown by Bukhtiyarov and Kaichev [8-9] that the relative population of these oxygen species depends on the silver cluster size. Moreover, the nucleophilic oxygen only appears for the particle sizes greater than 30 nm, indicating the relationship between the decrease in the rate of ethylene epoxidation on Ag/Al_2O_3 catalysts for silver particle sizes in the range of 30-50 nm and the disappearance of the nucleophilic oxygen.

The effect of silver particle size on the reaction rate has received considerable attention. Several researchers observed a catalytic size effect of silver particles within the range of 10-100 nm and correlated it to the changes in the particle morphology, surface structure, and the catalytic performance towards ethylene

epoxidation [7,10-17]. Mastikhin et al. [18] investigated the effect of particle size upon catalytic and electronic properties of supported Ag catalysts. The rate of ethylene epoxidation over Ag/Al_2O_3 catalysts dramatically increased to reach a maxima at a mean size of Ag particles about 40-50 nm. In 2005, Lu et al. [19] compared the particle size effect on ethylene and propylene epoxidations on a series of silver catalysts supported on $CaCO_3$. The large particles were shown to favor the ethylene epoxidation by 3-5 fold at 473-493 K, whereas the Ag particle size did not have a significant effect on propylene epoxidation. In addition, when the Ag particles became too small, they might be covered by a layer of Ag_2O, resulting in a lower selectivity for both ethylene and propylene epoxidation.

Besides the support selection, alkali metals (i.e. Cs and Na) [20-26], as well as organohalides which are widely used as feed additives (i.e. Cl) [27-28], have been added as promoters to improve the catalyst performance and the selectivity of the reaction. In real catalytic conditions, two types of Cs oxides (suboxide and peroxide) are employed for Cs-promoted Ag/Al_2O_3 catalysts. Their roles in silver-catalyzed ethylene epoxidation are different: suboxide promotes the ethylene epoxidation reaction while peroxide suppresses the total oxidation [29]. After that, Carvalho et al. [30] concluded that Cs promotional action is mainly due to geometric effects of improved silver dispersion. The increased Ag dispersion is believed to increase the amount of crystalline framework defects. Cs is believed to neutralize acid sites of the oxide support which are responsible for the isomerization of epoxide to acetaldehyde, followed by combustion reaction and also acts as a binder between the Ag and the support, resulting in a higher Ag coverage on the α-Al_2O_3 [31]. Fundamentally, the total oxidation of ethylene and ethylene oxide can occur on the Al_2O_3 surface. When Cs is added, it promotes a thin Ag film covering the Al_2O_3, resulting in the enhancement of the selectivity towards the ethylene epoxidation. Furthermore, Torres et al. [32] focused on the role of halogens as promoters for the silver-catalyzed partial oxidation of ethylene to ethylene oxide. The presence of co-adsorbed halogens was found to substantially decrease the energy barrier from the oxametallocycle intermediate (OMME) to EO, comparing with that from the same OMME intermediate to the undesired acetaldehyde (AC) product. They related the superior

activity of Cl to the additional presence of subsurface Cl that favors EO formation with respect to AC.

Bimetallic catalysts, composed of two distinct metal elements, are emerging as a new class of materials for various applications. In many cases, these catalysts can enhance some specific physical and chemical properties due to the synergistic effects. Pd-Ag bimetallic catalysts were reported to provide a better catalytic activity for ethylene oxide than the traditional monometallic silver catalysts [33-34]. Rojluechai et al. [35-36] revealed the effect of gold added on silver catalyst supported on high-surface-area alumina on the ethylene epoxidation activity. A small amount (0.63 wt.%) of added gold on the 13.18 wt.% Ag/Al_2O_3 catalyst could maximize ethylene epoxidation reaction. On the contrary, the formation of Au-Ag alloys at high gold loadings (higher than 0.63 wt.%) resulted in a decrease in the catalytic activity because the Au-Ag alloy favors a complete oxidation reaction. Indeed, some reports indicated that alloying Ag with Au influenced the bond strength of oxygen and the silver surface, resulting in modification of the relative population of the adsorbed species [37-38]. Recently, a large number of researches focused on bimetallic Cu-Ag catalysts which could improve the EO selectivity compared with pure silver catalysts [1,39-41]. Jankowiak and Barteau [42] observed that a small decrease of ethylene consumption in the activation energy (1-2 kcal/mol) was found in the bimetallic Cu-Ag catalysts relative to pure silver. Additionally, the bimetallic Cu-Ag catalysts were more selective for EO production with a comparable ethylene conversion over a wide range of reactant feed ratio than pure silver catalysts. The role of Cu in the bimetallic Cu-Ag catalyst is to alter the chemical and electronic properties of the surface. Cu changes the electronic properties of the binding sites which are available for oxametallocycle intermediates (and other adsorbates) to adsorb and alters the relative energies of the two transition states for the competing reactions of these intermediates. Copper addition increases the EO selectivity in the ways that it increases the relative difference between the barriers for the oxametallocycle ring-closure VS H-shift pathways, leading to more EO formation [43].

To prolong the stability of catalysts and maintain the high reaction selectivity, several approaches were reported such as Sn addition and CO_2 co-feeding [44-47]. Bae et al. [48] investigated the effect of tin on the product distribution and

catalyst stability in hydrodechlorination of CCl_4 over Pt-Sn/γ-Al_2O_3 catalyst. It was found that the addition of a moderate amount of tin to Pt/γ-Al_2O_3 catalyst improved the catalyst durability in the hydrodechlorination reaction and also enhanced the desired $CHCl_3$ selectivity. The enhancement in the stability results from the role of tin in decreasing the rate of carbonaceous species formation by destroying the large Pt ensemble sites which are responsible for the carbon deposition. Moreover, the improvement in the product distribution with the addition of a moderate amount of tin might be due to the electron transfer (changes in the electronic state of platinum particles) from tin to platinum so that the bond strength between platinum and hydrocarbons is weaken, resulting in the reduction of the binding energy of the intermediate species. As a result of that, the rate of coke formation is reduced, affecting the selectivity and the catalyst stability.

In our previous work [49-50], we studied the effect of various oxide supports ($Al_2O_{3,Acid}$, Al_2O_3 C, α-Al_2O_3, SiO_2, TiO_2 and $SrTiO_3$), as well as various mesoporous-assembled titanate supports (TiO_2, $MgTiO_3$, $CaTiO_3$, $SrTiO_3$, and $BaTiO_3$) synthesized via a sol-gel method with the aid of a structure-directing surfactant for Ag catalysts on EO selectivity and yield. Among of the studied catalysts, the 17.16 wt.% Ag supported on $SrTiO_3$ with the support calcination temperature of 923 K was the most effective catalyst for the ethylene epoxidation, enhancing the EO selectivity up to 99 % and yield of 4.7 %. The purpose of the present work was to improve the catalytic performance by adding various second metals (Au, Ba, Pd, Sn, and Cu) on the 17.16 wt.% Ag catalyst on the $SrTiO_3$ support, so called bimetallic catalysts, relative to those of pure silver and pure gold on the $SrTiO_3$ support in the epoxidation of ethylene. As mentioned before [50], the EO selectivity considerably dropped to 88 % after 36 h of operation. Therefore, the long-term stability of the best bimetallic catalyst (Cu-Ag) with added Sn as a promoter was investigated in this paper. Moreover, the catalytic performance of each studied catalyst was correlated with its physical and chemical properties.

6.3 Experimental

6.3.1 Materials

Silver nitrate ($AgNO_3$) was supplied by S.R. Lab. Tetraisopropyl orthotitanate (TIPT, $Ti(OCH(CH_3)_2)_4$), strontium nitrate ($Sr(NO_3)_2$), barium nitrate ($Ba(NO_3)_2$), copper nitrate trihydrate ($Cu(NO_3)_2 \cdot 3H_2O$), palladium chloride ($PdCl_2$), and laurylamine (LA, $CH_3(CH_2)_{11}NH_2$) were purchased from Merck. Acetylacetone (ACA, $CH_3COCH_2COCH_3$) was obtained from S.D. Fine-Chemical. Gold chloride trihydrate ($HAuCl_4 \cdot 3H_2O$) and tin chloride ($SnCl_2$) were supplied by Aldrich. Hydrochloric acid (HCl) and ethanol (C_2H_5OH) were purchased from Labscan. All chemicals used in this study were an analytical grade and used as received without further purification.

6.3.2 Catalyst preparation procedures

The nanocrystalline mesoporous-assembled $SrTiO_3$ support was synthesized via a sol-gel process with surfactant-assisted template in a TIPT/LA modified with ACA system [51-54]. Firstly, ACA was mixed with TIPT at an equimolar ratio. The mixed TIPT/ACA solution was gently shaken until homogeneous mixing. At the same time, a required amount of $Sr(NO_3)_2$ was dissolved in 24 ml of distilled water in a separate beaker. Then, ethanol was mixed with the as-prepared $Sr(NO_3)_2$ solution. After that, 1.112 g of the LA surfactant and 0.5 ml of HCl were added to obtain a $Sr(NO_3)_2$/LA/HCl solution. The $Sr(NO_3)_2$/LA/HCl solution was then poured into the TIPT/ACA solution. The final mixture was continuously stirred at room temperature until a homogeneous transparent sol was obtained. Next, the sol-containing solution was placed in an oven at 353 K for 4 d for complete gelation. Afterwards, the gel was dried at 353 K for 4 d to eliminate the solvents. The dried gel was finally calcined at 923 K to produce the desired mesoporous-assembled $SrTiO_3$ support. The mesoporous characteristic of this support was previously confirmed by Puangpetch et al. [52], showing a relatively narrow pore size distribution in the mesoporous region with a mean mesopore diameter of 3.5 nm and total pore volume of 0.047 $cm^3 \cdot g^{-1}$.

In this work, Ag catalysts were prepared by the incipient wetness impregnation using the $SrTiO_3$ support and silver nitrate precursor to achieve the nominal Ag loading of 17.5 wt.% (actual Ag loading = 17.16 wt.%) which was found to be the optimum Ag loading from our previous study [50], providing the maximum EO selectivity and yield. The same impregnation method was implemented for second metal loadings on the as-prepared Ag catalyst using different precursors ($HAuCl_4 \cdot 3H_2O$ for Au, $Cu(NO_3)_2 \cdot 3H_2O$ for Cu, $Ba(NO_3)_2$ for Ba, $PdCl_2$ for Pd, and $SnCl_2$ for Sn) to achieve various nominal second metal loadings of 0.25, 0.5, 0.75, 1, 1.5, and 2 wt.%. Then, the catalyst samples were dried at 383 K overnight, followed by calcination in air at 773 K for 5 h to produce the bimetallic catalysts.

Furthermore, the Cu-Ag bimetallic catalyst (the best catalyst as described later in Section 3.2) was further impregnated with a tin chloride precursor with various nominal tin loadings to investigate the effect of tin addition on the long-term stability of the catalyst. After the impregnation step, the catalyst samples were dried at 383 K overnight and then calcined at 673 K for 2 h to obtain the Sn-promoted Cu-Ag/$SrTiO_3$ catalyst [44].

6.3.3 Catalyst characterization techniques

The actual metal loadings on the synthesized $SrTiO_3$ catalysts were analyzed by an atomic absorption spectrophotometer (AAS, Varian, Spectr AA-300). The N_2 adsorption-desorption isotherms were obtained by a Brunauer-Emmett-Teller (BET) surface area analyzer (Quantachrome, SAA-1MP) to determine the specific surface areas of all studied catalysts. Each catalyst sample was firstly outgassed at 473 K for 8 h to remove the humidity and volatile species adsorbed on the surface.

An X-ray diffractometer (XRD, Rigaku, RINT 2200 HV) was used to identify the crystallinity of the synthesized catalysts. The diffractometer was equipped with a Ni filter and a Cu Kα radiation source (λ = 1.542 Å), operating at 40 kV and 30 mA. Each catalyst sample was scanned up to 2θ of 90° in a continuous scanning mode with a rate of 5° min^{-1}. The crystallite size of the studied catalysts was calculated by the Debye-Scherrer equation [55-56] from X-ray line broadening using the full line width at half maximum of intensity of X-ray peaks.

The catalyst surface morphologies were investigated by a field emission scanning electron microscope (FE-SEM, JEOL 5200-2AE). Prior to analysis, the samples were coated with Pt to improve their conductivity. The particle sizes of loaded metals and morphological surfaces of the catalyst samples were obtained by transmission electron microscopy (TEM, JEOL 3011 at 300 kV and JEOL 2010 at 200 kV). The specimens for TEM analysis were prepared by ultrasonically dispersing powders in ethanol and then placing drops of the suspension onto a grid coated with a carbon film. The existence of Ag and other second metal particles on the $SrTiO_3$ support was verified by using an energy dispersive X-ray spectroscope (EDS) attached to the TEM. The metal particle sizes were determined from statistical data of the TEM images.

The oxygen and ethylene uptakes of the investigated catalysts were examined using a temperature-programmed desorption (TPD) analyzer (Quantachrome, Chembet 3000). Initially, oxygen (4.99 % O_2 in He) or pure ethylene (99.99 % C_2H_4) was allowed to adsorb onto the catalyst surface at 473 K for 2 h for the TPD experiments. Then, the catalyst samples were cooled down to room temperature in a high-purity of He stream. After that, the catalyst samples were heated from room temperature up to 1173 K with a heating rate of 10 K/min, and the desorbed gas was swept by a high-purity He at a flow rate of 20 cm^3/min. A thermal conductivity detector (TCD) was used to determine the desorption profiles which were used to calculate both oxygen and ethylene uptakes.

The oxidation states of the loaded metals were analyzed by an X-ray photoelectron spectroscope (XPS, Shimadzu, Kratos). A monochromatic Al Kα source was used as the X-ray source. The relative surface charging of the samples was removed by referencing all the energies to the C1s level as an internal standard at 284.8 eV [57]. The coke formation on the spent catalysts was quantified by using a thermogravimetric and differential thermal analyzer (TG-DTA, PerkinElmer, Pyris Diamond).

6.3.4 Activity testing experiments

The ethylene epoxidation reaction experiments over various monometallic and bimetallic catalysts on the $SrTiO_3$ support were conducted in a packed-bed 8-mm ID tubular reactor at 24.7 psia and the reaction temperature was varied from 498 to 563 K. An amount of 30 mg of catalyst powder was initially pretreated with oxygen at 473 K for 2 h. The feed gas was a mixture of 40 % ethylene in He, pure oxygen (HP grade), and pure helium (HP grade). The feed gas composition of 6 % ethylene and 6 % oxygen with helium balance was achieved by using mass flow controllers. During the reaction testings, the space velocity through the reactor was maintained at 6,000 h^{-1} for all studied catalysts. An on-line gas chromatograph (Perkin Elmer, ARNEL) equipped with a 60/80 CARBOXEN 1 packed column (capable of separating carbon dioxide, ethylene, and oxygen) and a Rt-U PLOT capillary column (capable of separating EO, ethane, and propane) was used to analyze the compositions of the feed and product gases. The amount of acetaldehyde was found in trace for all experimental runs because of further oxidation to carbon dioxide and water [58]. The catalytic activity of each studied catalyst was compared at 6 h in operation. The experimental data with less than 5 % error were averaged to assess the catalytic performance. Moreover, the system was operated up to 72 h for the best bimetallic catalyst with and without Sn promoter in comparison with Ag catalyst to observe the long-term stability of these catalysts.

6.4 Results and Discussion

6.4.1 Catalyst characterization results

6.4.1.1 XRD results

The XRD patterns of various pure (Ag, Au) and bimetallic (Au-Ag, Ba-Ag, Pd-Ag, Sn-Ag, Cu-Ag, and Sn-promoted Cu-Ag) catalysts on the $SrTiO_3$ support at their optimum metal loadings (based on the highest EO selectivity and yield) are shown in Figure 6.1. The dominant peaks of metallic silver at 2θ of about 28°, 38°, and 44° correspond to (110), (111), and (200) planes. An extremely small Ag_2O peak was observed at 2θ of 35°. The peaks of metallic silver (2θ of 28°, 38°, and 44°) were superimposed by those of metallic gold, while metallic copper

was present at 2θ of 30° and 44° and at 2θ of 42° for barium. No crystalline phase of palladium or tin was detected in the Pd-Ag and Sn-Ag bimetallic catalysts, as well as Sn-promoted on Cu-Ag bimetallic catalyst. This might be because the amounts of both palladium and tin were too low to be detected by XRD. The XRD results point out that silver and second metals were mostly in their metallic forms. In a comparison with the pure Ag catalyst, the pure Au and all bimetallic catalysts (except Sn-Ag and Sn-promoted on Cu-Ag catalysts) showed higher crystalline structures of the loaded Ag and the $SrTiO_3$ support. The results suggest that the presence of tin even at the low concentration range of 0.32-0.44 wt.% can almost completely change the crystalline structure of the $SrTiO_3$ to amorphous form (see the disappearance of Ag peaks).

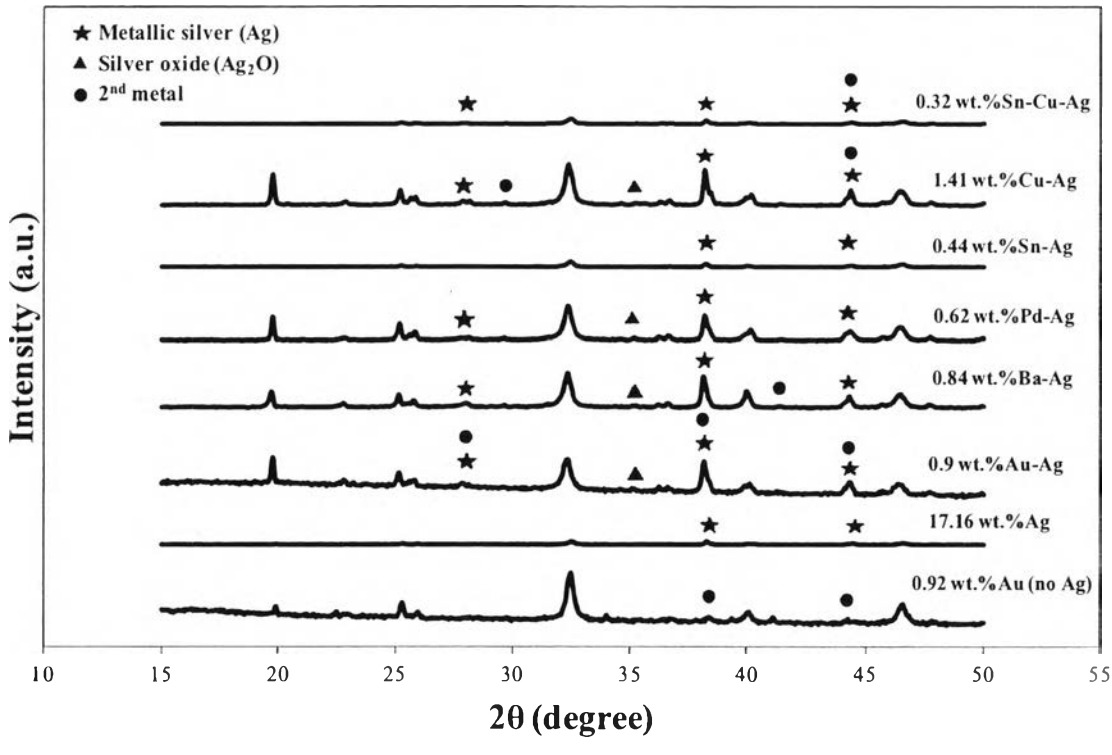

Figure 6.1 XRD patterns of all studied catalysts on the $SrTiO_3$ support at their optimum metal loadings with 17.16 wt.% Ag.

6.4.1.2 Specific surface area results

The measured specific surface areas of all studied catalysts at their optimum catalyst loadings are comparatively shown in Table 6.1. The specific surface area of the Ag catalyst with any added second metal slightly dropped, meaning that the addition of any second metal does not significantly affect the specific surface area of the Ag catalyst on the $SrTiO_3$ support. Among the investigated catalysts, both bimetallic Ba-Ag and Pd-Ag catalysts possessed the lowest specific surface area, followed by the Sn-promoted on Cu-Ag catalyst. The highest specific surface area of 2.4 m^2/g was obtained from the 0.92 wt.% $Au/SrTiO_3$ catalyst. The results can be concluded that the addition of different types and loadings of all catalysts did not significantly affect the specific surface area property of the $SrTiO_3$ support.

6.4.1.3 Surface morphology

Figure 6.2 shows the surface morphology of all investigated catalysts on the $SrTiO_3$ support. The changes in the surface morphologies can be clearly seen for all catalysts after the addition of any second metal, especially for Au-loaded catalysts (both Au and Au-Ag catalysts). The SEM images confirm the existence of the small second metal particles, as well as pure Au and pure Ag particles randomly dispersed throughout the catalysts. Moreover, an addition of small amount of tin on the Cu-Ag catalyst also altered the surface topology as illustrated in the Figure 6.2g and 6.2h.

Table 6.1 Characteristics of pure Ag, pure Au and bimetallic catalysts on the $SrTiO_3$ support at their own optimum metal loadings (corresponding to the highest ethylene epoxidation activity)

Actual Ag loading (wt.%)	Actual 2nd metal loading (wt.%)	Specific surface area (m^2/g)	Ag particle size[a] (nm)	2nd metal particle size[a] (nm)	O_2 uptake[b] ($\mu mol\ g^{-1}$)	C_2H_4 uptake[b] ($\mu mol\ g^{-1}$)
17.16	0	1.5	59	-	5155	6308
0	0.92 Au	2.4	-	6.6	3979	5064
17.16	0.9 Au	1.3	59	4.5	4417	5412
17.16	0.84 Ba	0.7	59	5.2	9034	5783
17.16	0.62 Pd	0.7	59	5.8	4037	4975
17.16	0.44 Sn	1.4	59	3.2	1408	4851
17.16	1.41 Cu	1.1	58	4.7	6935	5767
17.16	0.32 Sn*-1.39 Cu	0.8	58	2.8 (Sn*), 5.5 (Cu)	7429	6065

[a] From TEM analysis
[b] calculated in the temperature range of 400 to 700 K
* Sn-promoted on Cu-Ag bimetallic catalyst

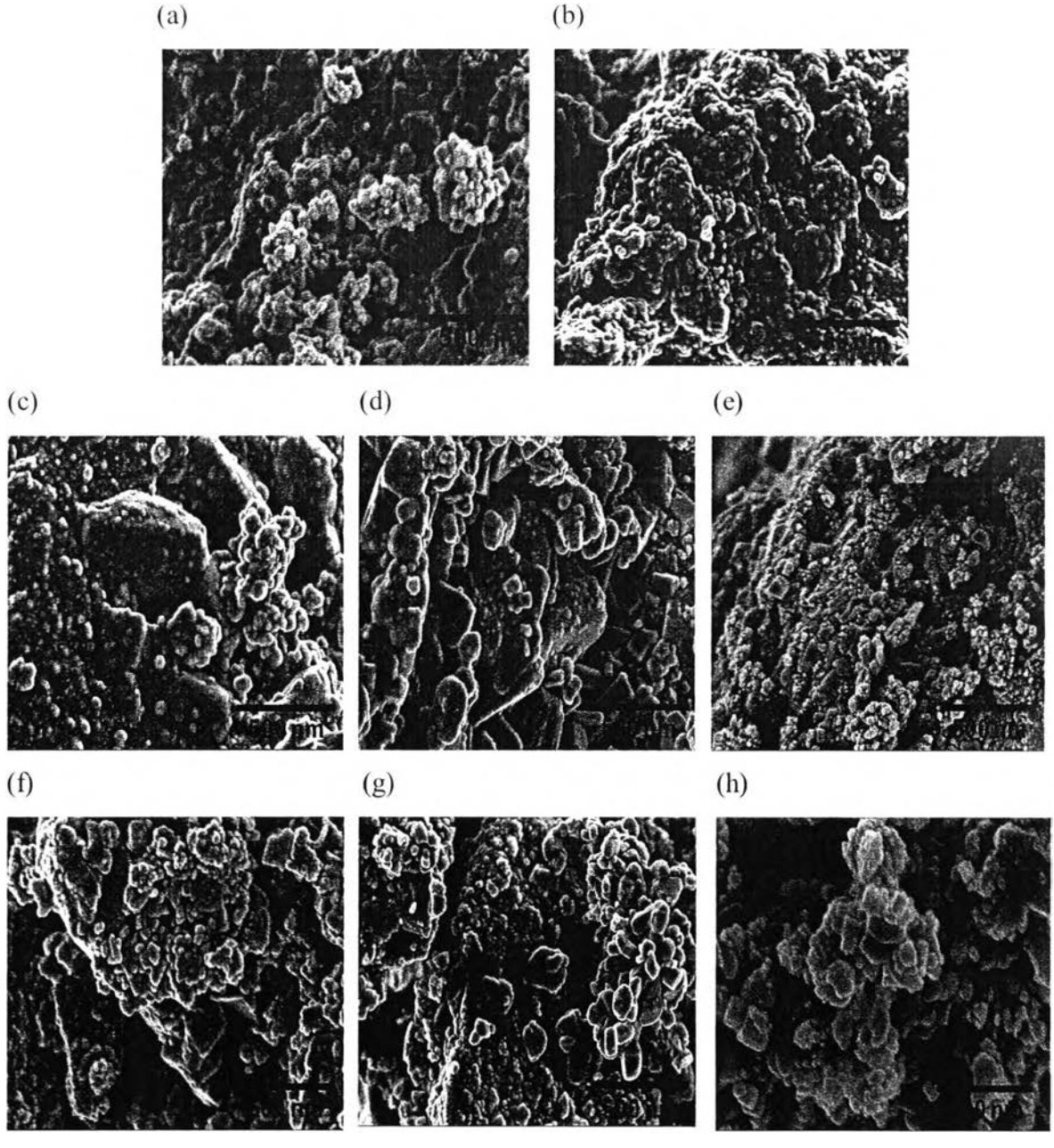

Figure 6.2 SEM images of all investigated catalysts on the $SrTiO_3$ support (a) 17.16 wt.% Ag, (b) 0.92 wt.% Au, (c) 0.9 wt.% Au-17.16 wt.% Ag, (d) 0.84 wt.% Ba-17.16 wt.% Ag, (e) 0.62 wt.% Pd-17.16 wt.% Ag, (f) 0.44 wt.% Sn-17.16 wt.% Ag, (g) 1.41 wt.% Cu-17.16 wt.% Ag, and (h) 0.32 wt.% Sn-1.39 wt.% Cu-17.16 wt.% Ag catalysts (70,000x).

Figure 6.3 displays the inhomogeneous dispersion of metal nanoparticles of the selected catalysts (providing the high EO activity) on the surface

of the $SrTiO_3$ support. The presence of very small tin particles (2.8 nm) on the Cu-Ag bimetallic catalyst was observed randomly (Figure 6.3e), suggesting that the added tin was in a single crystalline structure as confirmed by the SAD result (not shown here). The average sizes of metal nanoparticles of all prepared catalysts are summarized in Table 6.1. It was found that the addition of any second metal had no significant effect on the Ag particle sizes in all studied catalysts. The monometallic 0.92 wt.% $Au/SrTiO_3$ catalyst had the largest average gold particle size (6.6 nm), while the smallest average metal particle size (2.8 nm) of tin was found on the 0.32 wt.% Sn-1.39 wt.% Cu-17.16 wt.% $Ag/SrTiO_3$ catalyst. After the reaction experiments, the average Ag particle size increased from 58 nm for the fresh catalyst to 62 nm for the spent catalyst, while the average Cu particle size increased from 4.7 to 5.8 nm for the 1.41 wt.% Cu-17.16 wt.% $Ag/SrTiO_3$ catalyst without Sn promoter. On the other hand, for the 1.39 wt.% Cu-17.16 wt.% $Ag/SrTiO_3$ catalyst with 0.32 wt.% Sn promoter, the average Ag particle size increased from 58 nm for the fresh catalyst to 61 nm for the spent catalyst while the average Cu particle size slightly increased from 5.5 to 5.9 nm and the average Sn particle sizes were about the same at 2.8 nm. The results imply that a very small of Sn promoter does not significantly alter the physical sizes of both Ag and Cu particles after the epoxidation reaction testing.

6.4.1.4 TPD results

Table 6.1 shows both oxygen and ethylene uptakes which were used to relate to the catalytic activity towards the ethylene epoxidation reaction in this study. The uptake results of both oxygen and ethylene were calculated based on the oxygen and ethylene desorption peaks at the temperature range of 400-700 K in which EO was found to present in the product gas. The highest oxygen uptake was obtained from the 0.84 wt.% Ba-17.16 wt.% $Ag/SrTiO_3$ catalyst (9034 $\mu mol\ g^{-1}$), followed by the 0.32 wt.% Sn-1.39 wt.% Cu-17.16 wt.% Ag catalyst (7429 $\mu mol\ g^{-1}$), whereas the lowest oxygen uptake was obtained from the 0.44 wt.% Sn-17.16 wt.% $Ag/SrTiO_3$ catalyst (1408 $\mu mol\ g^{-1}$). The ethylene uptakes were comparably high for all catalysts, except those of the 0.92 wt.% Au, 0.62 wt.% Pd-17.16 wt.% Ag, and 0.44 wt.% Sn-17.16 wt.% Ag catalysts on the $SrTiO_3$ supports.

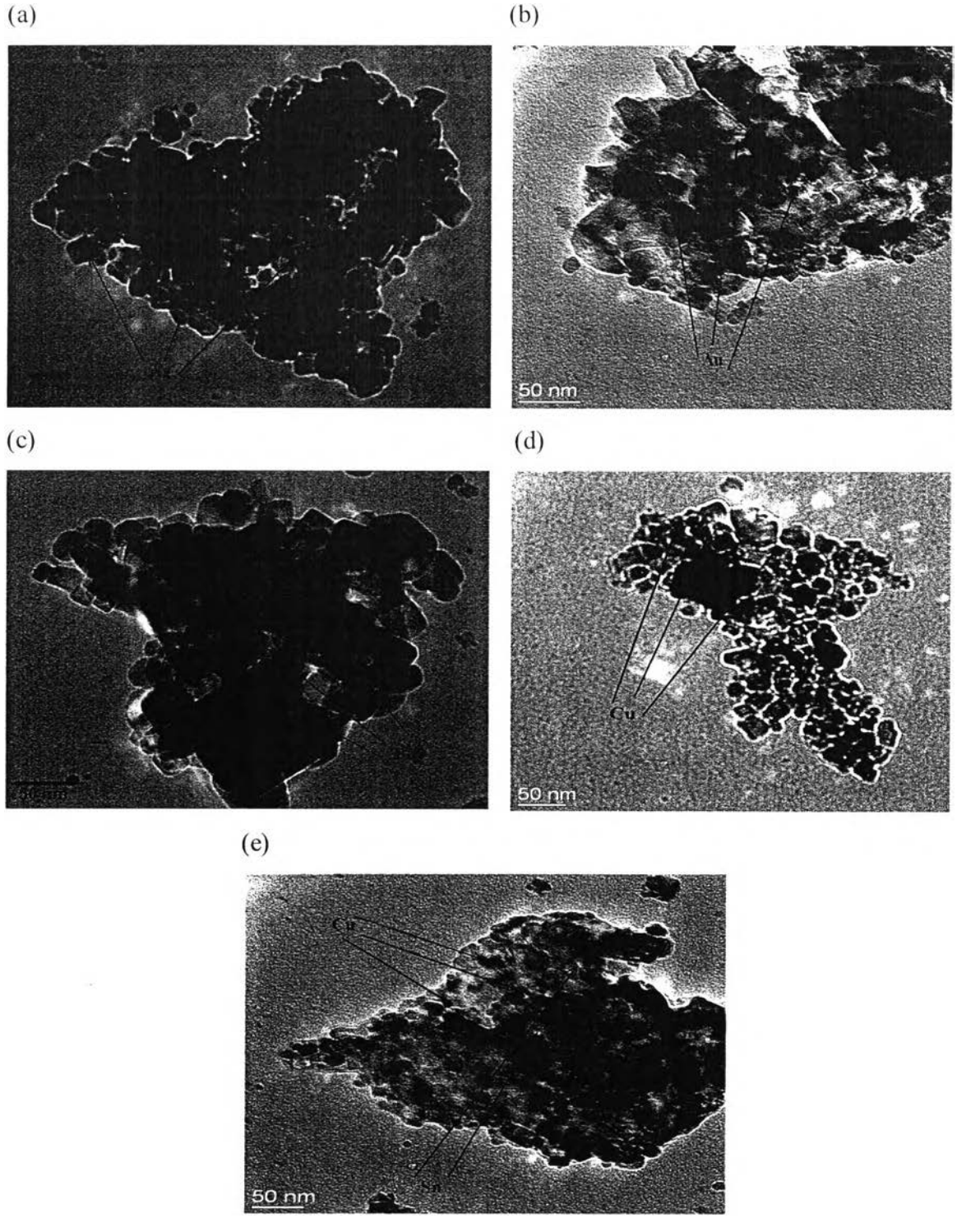

Figure 6.3 TEM-EDS images of selected catalysts on $SrTiO_3$ support (a) 17.16 wt.% Ag, (b) 0.9 wt.% Au-17.16 wt.% Ag, (c) 0.84 wt.% Ba-17.16 wt.% Ag, (d) 1.41 wt.% Cu-17.16 wt.% Ag, and (e) 0.32 wt.% Sn-1.39 wt.% Cu-17.16 wt.% Ag catalysts.

Interestingly, the tin loading on the Cu-Ag/$SrTiO_3$ catalyst showed the synergistic effect in terms of both uptakes, especially the oxygen uptake by increasing the oxygen uptake from 6935 to 7429 μmol g^{-1} which will be used to explain why the addition of Sn promoter could enhance the long-term stability of the bimetallic Cu-Ag catalyst later.

6.4.1.5 XPS results

Table 6.2 summarizes the XPS results of all studied catalysts on the $SrTiO_3$ support at their own optimum metal loadings. The existence of both metallic and metal oxide forms of all studied metals was verified by their binding energies [57]. However, the amounts of metallic Pd and Sn, together with their oxide forms cannot be detected by the XPS technique because of the small amounts of metal loadings. The XPS results suggest that all studied catalysts on the $SrTiO_3$ support mainly composed of metallic forms. The highest molar ratio of metallic Ag to Ag_2O of 14.4:1 was found on the 0.32 wt.% Sn-1.39 wt.% Cu-17.16 wt.% Ag/$SrTiO_3$ catalyst before the reaction and it slightly decreased to 11.2:1 after the reaction. The molar ratio of metallic Ag to Ag_2O of the 1.41 wt.% Cu-17.16 wt.% Ag/$SrTiO_3$ catalyst decreased significantly from 11.5:1 to 5.4:1 after the reaction. The lowest portion of metallic form was obtained from the 0.84 wt.% Ba-17.16 wt.% Ag/$SrTiO_3$ catalyst before the reaction but the 1.41 wt.% Cu-17.16 wt.% Ag/$SrTiO_3$ possessed the lowest fraction (2.8:1) after the reaction. Interestingly, the incorporation of tin with a proper amount showed the significant ability to maintain the metallic forms of both Ag and Cu during the epoxidation reaction testing. The reduction of ethylene epoxidation reaction performance in the relation to the increase in metal oxide fractions of all studied catalysts will be further discussed later.

Table 6.2 XPS results of all studied catalysts on $SrTiO_3$ support at their own optimum metal loadings

Actual Ag loading (wt.%)	Actual 2nd metal loading (wt.%)	Metallic Ag : Ag_2O molar ratio	Metallic metal : metal oxide of second metal
17.16	0	9.5 : 1	-
0	0.92 Au	0 : 0	100 : 0
17.16	0.9 Au	7.9 : 1	100 : 0
17.16	0.84 Ba	5.9 : 1	9.4 : 1
17.16	0.62 Pd	7.4 : 1	-
17.16	0.44 Sn	5.9 : 1	-
17.16	1.41 Cu	11.5 : 1	14.9 : 1
	(after reaction)	(5.4 : 1)	(2.8 : 1)
17.16	0.32 Sn*-1.39 Cu	14.4 : 1	15.7 : 1
	(after reaction)	(11.2 : 1)	(10.6 : 1)

* Sn-promoted on Cu-Ag bimetallic catalyst
(after reaction) = same catalyst after the reaction

6.4.1.6 TG-DTA results

The amounts of coke formation on the spent catalysts after the epoxidation of ethylene at 6 h and 72 h are summarized in Table 6.3. The 0.62 wt.% Pd-17.16 wt.% $Ag/SrTiO_3$ catalyst possessed the highest coke formation at both operation time intervals (7.7 % at 6 h and 10.1 % at 72 h) while the 0.32 wt.% Sn-promoted on 1.39 wt.% Cu-17.16 wt.% Ag catalyst had the lowest amounts of coke (1.7 % at 6 h and 2.9 % at 72 h). The results suggest that the addition of both Cu and Sn as the second metal and the promoter can significantly reduce the coke formation on the Ag catalyst corresponding to an ability to maintain the high catalytic activity towards the ethylene epoxidation which will be further discussed.

Table 6.3 Coke formation on the spent Ag-loaded catalysts with different second metals and Sn promoter after 6 h and 72 h on stream of the ethylene epoxidation reaction (6% O_2 and 6% C_2H_4 balanced with He, a space velocity of 6000 h^{-1}, a pressure of 24.7 psia, a reaction temperature of 548 K)

Optimum Ag loading (wt.%)	Optimum 2nd metal loading (wt.%)	Coke formation at 6 h (wt.%)	Coke formation at 72 h (wt.%)
17.16	0	3.3	5.1
0	0.92 Au	4.8	9.3
17.16	0.9 Au	5.2	8.7
17.16	0.84 Ba	6.5	8.2
17.16	0.62 Pd	7.7	10.1
17.16	0.44 Sn	3.0	4.5
17.16	1.41 Cu	2.4	4.0
17.16	0.32 Sn-1.39 Cu	1.7	2.9

6.4.2 Ethylene epoxidation activity results

Regarding to our previous work [49-50], the $Ag/SrTiO_3$ catalyst with the support calcination temperature of 923 K and the Ag loading of 17.16 wt.% exhibited the superior catalytic activity in terms of the maximum EO selectivity of 99.12 % and the highest EO yield of 4.7 %. In the present work, the catalytic performance of this Ag catalyst loaded on the $SrTiO_3$ support was further improved by adding various second metals (Au, Ba, Pd, Sn, and Cu). Figure 6.4 illustrates the ethylene epoxidation reaction performance as a function of reaction temperature and second metal type at the optimum loading of each second metal based on 6 h on stream. For any given bimetallic catalyst, an increment of temperature resulted in the increment of EO yield and reached a maximum at 548 K. However, the EO yield substantially dropped with further increasing reaction temperature from 548 to 563 K. The reduction of EO yield of each studied catalyst was found to correspond to the increase in the complete oxidation to CO_2 at a higher temperature [58-59].

(a)

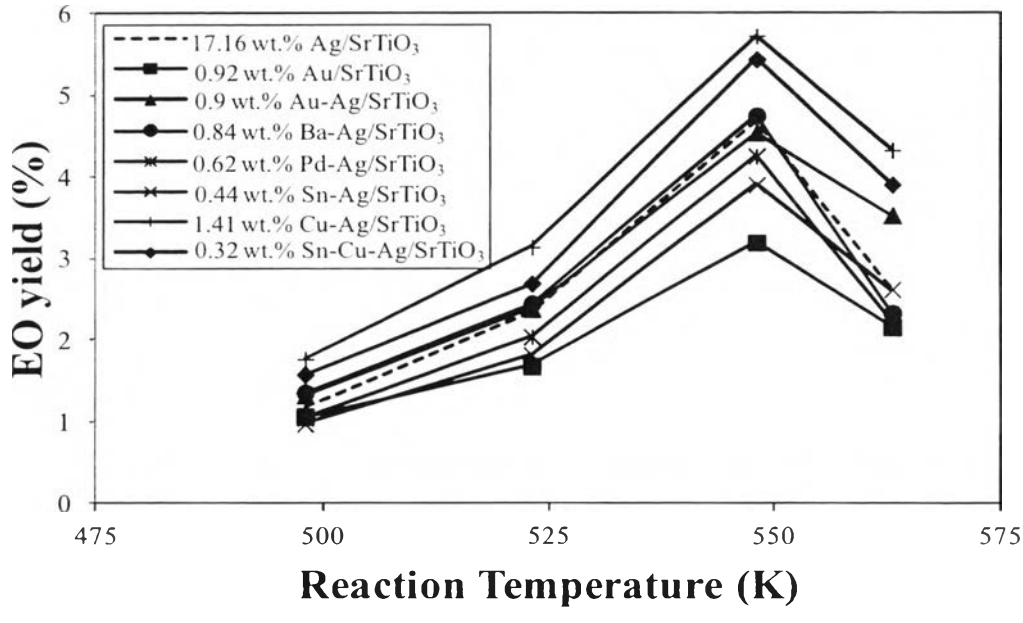

(b)

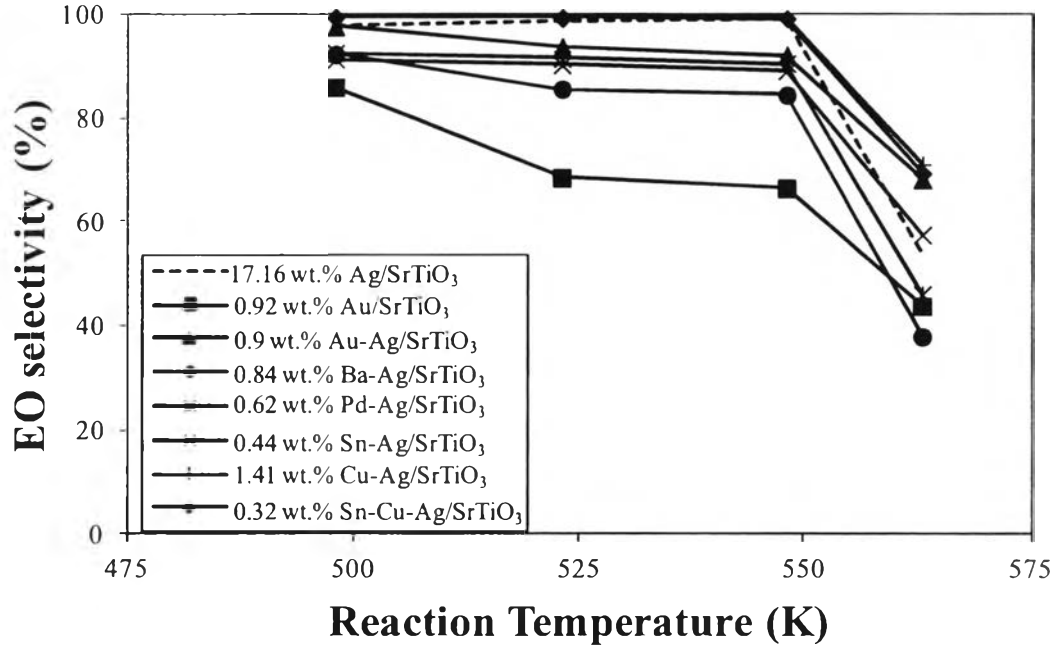

Figure 6.4 (a) EO yield and (b) EO selectivity as a function of reaction temperatures of the studied catalysts on 17.16 wt.% $Ag/SrTiO_3$ with various second metals as compared to the $Au/SrTiO_3$ and the 0.32 wt.% Sn-1.39 wt.% Cu-17.16 wt.% $Ag/SrTiO_3$ at 6 h on stream (6% O_2 and 6% C_2H_4 balanced with He, a space velocity of 6000 h^{-1}, a pressure of 24.7 psia).

From the EO selectivity results, the addition of second metal except Cu showed a negative effect in which the EO selectivity decreased with increasing reaction temperature while the presence of 1.41 wt.% Cu on the 17.16 wt.% $Ag/SrTiO_3$ catalyst could slightly increase the EO selectivity up to a reaction temperature of 548 K. However, both EO selectivity and yield of all studied catalysts decreased markedly with further increasing reaction temperature beyond 548 K.

Among the investigated catalysts, the 1.41 wt.% Cu-17.16 wt.% $Ag/SrTiO_3$ catalyst provided the highest EO yield of 5.7 %, as well as the maximum EO selectivity of 99.27 % at the optimum reaction temperature of 548 K. As a result of that, this catalyst was selected to explore the promotional effect of tin on the improvement of the catalytic activity and the long-term stability. It was found that the EO yield and EO selectivity were slightly lowered to 5.4 % and 99.2 % after an addition of tin on the bimetallic Cu-Ag catalyst (0.32 wt.% Sn-1.39 wt.% Cu-17.16 wt.% $Ag/SrTiO_3$ catalyst). On the contrary, the worst catalytic performance was obtained from the monometallic 0.92 wt.% $Au/SrTiO_3$ catalyst, giving only 66.5 % of EO selectivity and 3.2 % of EO yield. The catalytic performance was found to improve over the bimetallic Au-Ag catalyst, enhancing the EO selectivity up to 92 % as compared with the monometallic Au catalyst. For the monometallic Ag catalyst, the EO selectivity was comparably high in the temperature range of 498-548 K but significantly dropped after that. The ethylene epoxidation activity of all studied catalysts at 6 h and 72 h on stream is summarized in Table 6.4. For the long-term activity and stability, all studied catalysts were operated up to 72 h. After 72 h of the reaction, the catalytic activities of all studied catalysts declined significantly (data not shown here). The reduction of the catalytic activities of all studied catalysts can be correlated with the coke formation on the spent catalysts (Table 6.3) which reduced the active sites for the EO formation reaction, leading to a higher CO_2 selectivity in the product gas, as found experimentally which is in a good agreement with literature [48].

Table 6.4 Ethylene epoxidation activity of all studied catalysts at 6 h and 72 h on stream (6% O_2 and 6% C_2H_4 balanced with He, a space velocity of 6000 h^{-1}, a pressure of 24.7 psia, and optimum reaction temperature of 548 K)

Actual Ag loading (wt.%)	Actual 2nd metal loading (wt.%)	6 h of time on stream		72 h of time on stream	
		EO selectivity (%)	EO yield (%)	EO selectivity (%)	EO yield (%)
17.16	0	99.1	4.7	88.1	3.4
0	0.92 Au	66.5	3.2	47.9	1.8
17.16	0.9 Au	92.2	4.6	80.6	3.2
17.16	0.84 Ba	84.5	4.8	69.3	3.3
17.16	0.62 Pd	90.6	4.3	79.5	2.8
17.16	0.44 Sn	89.2	3.9	85.2	3.2
17.16	1.41 Cu	99.3	5.7	90	4.5
17.16	0.32 Sn-1.39 Cu	99.2	5.4	95.1	5.2

The long-term stability (72 h of operation) in terms of EO yield and EO selectivity of the best bimetallic catalyst (1.41 wt.% Cu-17.16 wt.% Ag) with (0.32 wt.% Sn) and without Sn promoter is compared with the traditional monometallic Ag catalyst on the $SrTiO_3$ support at the reaction temperature of 548 K, as shown in Figure 6.5. The activities of all studied catalysts remained stable after 44 h of operation. The EO selectivity of the 17.16 wt.% Ag catalyst was similar to the other two catalysts up to 8 h of operation but it dropped dramatically to reach a minimum of both EO selectivity and yield beyond 44 h of operation. The bimetallic 1.41 wt.% Cu-17.16 wt.% Ag catalyst showed better long-term stability until 18 h of operation which the activity started to drop rapidly to 4.5 % of EO yield and 90 % of EO selectivity at 72 h of operation. Interestingly, the long-term stability of the bimetallic 1.41 wt.% Cu-17.16 wt.% Ag catalyst was significantly enhanced by an addition of Sn promoter (0.32 wt.%), resulting in the high EO yield of 5.2 % and EO selectivity up to 95 % at 72 h of operation. The best catalytic performance especially for the long-term activity and stability of the bimetallic 1.39 wt.% Cu-17.16 wt.% $Ag/SrTiO_3$ catalyst with 0.32 wt.% Sn promoter may be correlated to the high oxygen and ethylene uptakes, indicating the high opportunity for the reactants (oxygen and ethylene) to react together to form ethylene oxide (Table 6.1). The largest fraction of metallic Ag (Table 6.2) might help to facilitate the epoxidation reaction [7]. Moreover, tin addition as a promoter was found to prolong the stability of the Cu-Ag catalyst, resulting from decreasing of the rate of carbonaceous species formation as well as the reduction of the binding energy of the intermediate species by tin [48] as confirmed by the TG-DTA result (Table 6.3).

(a)

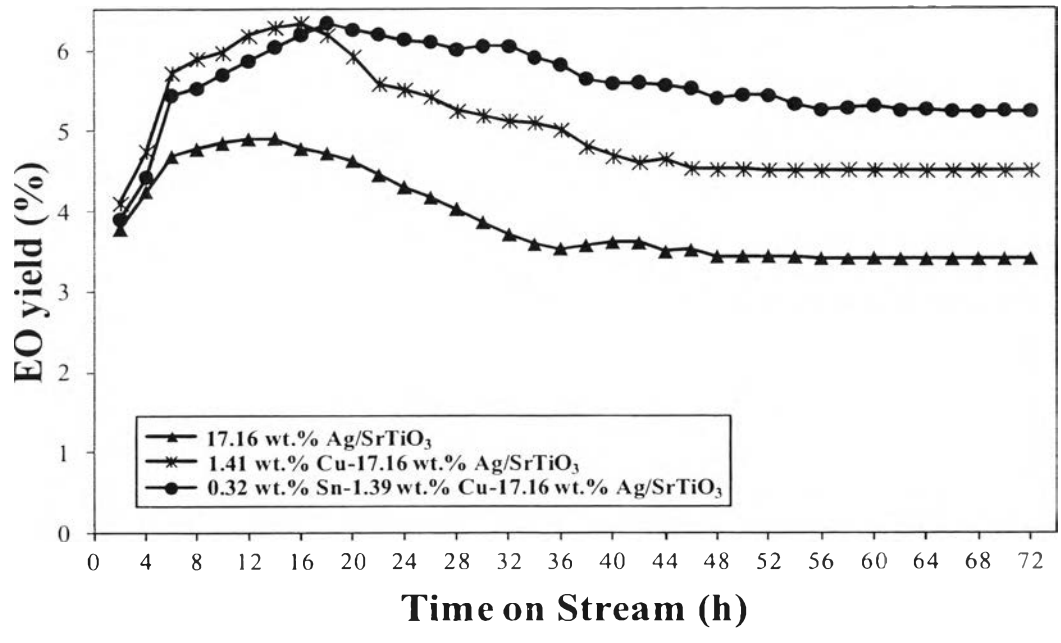

(b)

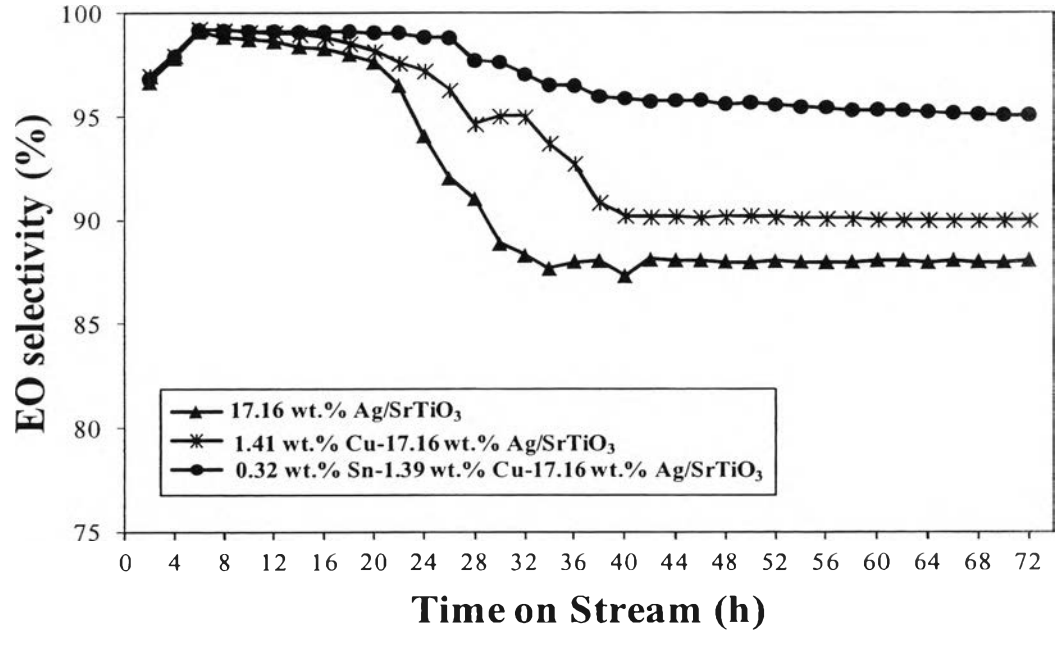

Figure 6.5 EO yield (a) and EO selectivity (b) as a function of time on stream for 17.16 wt.% $Ag/SrTiO_3$ catalyst compared with 1.41 wt.% Cu-17.16 wt.% $Ag/SrTiO_3$ catalyst and 0.32 wt.% Sn-1.39 wt.% Cu-17.16 wt.% $Ag/SrTiO_3$ catalyst (6% O_2 and 6% C_2H_4 balanced with He, a space velocity of 6000 h^{-1}, a pressure of 24.7 psia, a reaction temperature of 548 K).

6.5 Conclusions

Among the investigated catalysts, the bimetallic Cu-Ag catalyst significantly improved the catalytic performance of the traditional monometallic Ag catalyst on the $SrTiO_3$ support by increasing Ag metallic fraction, leading to decreasing coke formation. The 0.32 wt.% Sn loaded on 1.39 wt.% Cu-17.16 wt.% $Ag/SrTiO_3$ was found to provide the highest EO yield of 5.2 %, the maximum EO selectivity of 95.1 % for the long-term operation (72 h). The addition of Sn promoter with a proper amount on the bimetallic Cu-Ag catalyst was found to increase both oxygen uptake and the Ag metallic fraction, leading to a reduction of coke formation. As a consequence, the ethylene epoxidation reaction was significantly enhanced especially for a long-term operation.

6.6 Acknowledgements

This work was supported by The Royal Golden Jubilee Ph.D. Program (RGJ-Industry) awarded by The Thailand Research Fund with the in-kind support from PTT Global Chemical Public Co. Ltd.; the Sustainable Petroleum and Petrochemicals Research Unit, Center of Excellence on Petrochemical and Materials Technology, Chulalongkorn University (Thailand); and the Transportation Energy Center, Department of Chemical Engineering, University of Michigan (USA).

6.7 References

[1] S. Piccinin, C. Stampfl, Phys. Rev. B 77 (2008) 1-9.

[2] R.A.V. Santen, H.P.C.E. Kuipers, Adv. Catal. 35 (1987) 1-57.

[3] H.J. Lee, M. Ghanta, D.H. Busch, B. Subramaniam, Chem. Eng. Sci. 65 (2010) 128-134.

[4] S. Linic, J. Jankowiak, M.A. Barteau, J. Catal. 224 (2004) 489-493.

[5] K. Weissermel, Industrial Organic Chemistry, Wiley-VCH, 2003, pp. 145-152.

[6] P. Christopher, S. Linic, ChemCatChem. 2 (2010) 78.

[7] S.N. Goncharova, E.A. Paukshtis, B.S. Bal'zhinimaev, Appl. Catal., A 126 (1995) 67-84.

[8] V.I. Bukhtiyarov, V.V. Kaichev, J. Mol. Catal. A: Chem. 158 (2000) 167-172.

[9] V.I. Bukhtiyarov, A.F. Carley, L.A. Dollard, M.W. Roberts, Surf. Sci. 381 (1997) 605-608.

[10] M. Jarjoui, B. Moraveck, P.C. Gravelle, S.J. Teichner, J. Chim. Phys. 75 (1978) 1061.

[11] M. Jarjoui, P.C. Gravelle, S.J. Teichner, J. Chim. Phys. 75 (1978) 1069.

[12] S.R. Seyedmonir, J.K. Plischke, M.A. Vannice, H.W. Young, J. Catal. 123 (1990) 534.

[13] P. Harriot, J. Catal. 21 (1971) 56.

[14] S. Cheng, A. Clearfield, J. Catal. 94 (1985) 455.

[15] J.C. Wu, P. Harriot, J. Catal. 39 (1975) 395.

[16] X.E. Verykios, F.P. Stein, R.W. Couglin, J. Catal. 66 (1980) 368.

[17] J.K. Lee, X.E. Verykios, R. Pitchai, Appl. Catal. 50 (1989) 171-188.

[18] V.M. Mastikhin, S.N. Goncharova, V.M. Tapilin, V.V. Terskikh, B.S. Balzhinimaev, J. Mol. Catal. A: Chem. 96 (1995) 175-179.

[19] J. Lu, J.J. Bravo-Suarez, A. Takahashi, M. Haruta, S.T. Oyama, J. Catal. 232 (2005) 85-95.

[20] R.B. Grant, R.M. Lambert, Langmuir 1 (1985) 29-33.

[21] W.S. Epling, G.B. Hoflund, D.M. Minahan, J. Catal. 171 (1997) 490-497.

[22] G.B. Hoflund, D.M. Minahan, J. Catal. 162 (1996) 48-53.

[23] D.M. Minahan, G.B. Hoflund, J. Catal. 158 (1996) 109-115.

[24] Ch. Karavasilis, S. Bebelis, C.G. Vayenas, J. Catal. 160 (1996) 205-213.

[25] P. Yinsheng, Z. Shi, Catal. Lett. 12 (1992) 307-318.

[26] J.C. Dellamorte, J. Lauterbach, M.A. Barteau, Catal. Today 120 (2007) 182-185.

[27] K.L. Yeung, A. Gavriilidis, A. Varma, M.M. Bhasin, J. Catal. 174 (1998) 1-12.

[28] D. Lafarga, A. Varma, Chem. Eng. Sci. 55 (2000) 749-758.

[29] E.A. Podgornov, I.P. Prosvirin, V.I. Bukhtiyarov, J. Mol. Catal. A: Chem. 158 (2000) 337-343.

[30] C.N. Marta, F.B. Passos, M. Schmal, J. Catal. 248 (2007) 124-129.

[31] D.M. Minahan, G.B. Hoflund, W.S. Epling, D.W. Schoenfeld, J. Catal. 168 (1997) 393-399.

[32] D. Torres, F. Illas, R.M. Lambert, J. Catal. 260 (2008) 380-383.

[33] V.G. Nenajdenko, A.Y. Vasilkov, A.A. Goldberg, V.M. Muzalevskiy, A.V. Naumkin, V.L. Podshibikhin, A.V. Shastin, E.S. Balenkova, Mendeleev Commun. 20 (2010) 200-202.

[34] J.C. Dellamorte, J. Lauterbach, M.A. Barteau, Appl. Catal., A 391 (2011) 281-288.

[35] S. Rojluechai, S. Chavadej, J.W. Schwank, V. Meeyoo, J. Chem. Eng. Jpn. 39 (2006) 321-326.

[36] S. Rojluechai, S. Chavadej, J.W. Schwank, V. Meeyoo, Catal. Commun. 8 (2007) 57-64.

[37] D.I. Kondarides, X.E. Verykios, J. Catal. 158 (1996) 363-377.

[38] S. Piccinin, S. Zafeiratos, C. Stampfl, T.W. Hansen, M. Havecker, D. Teschner, V.I. Bukhtiyarov, F. Girgsdies, A. Knop-Gericke, R. Schlogl, M. Scheffler, Phys. Rev. Lett. 104 (2010) 1-4.

[39] D. Torres, N. Lopez, F. Illas, J. Catal. 243 (2006) 404-409.

[40] S. Piccinin, N.L. Nguyen, C. Stampfl, M. Scheffler, J. Mater. Chem. 20 (2010) 10521-10527.

[41] N.L. Nguyen, S. Piccinin, S. Gironcoli, J. Phys. Chem. C 115 (2011) 10073-10079.

[42] J.T. Jankowiak, M.A. Barteau, J. Catal. 236 (2005) 366-378.

[43] J.T. Jankowiak, M.A. Barteau, J. Catal. 236 (2005) 379-386.

[44] S.M. Lima, A.M. Silva, G. Jacobs, B.H. Davis, L.V. Mattos, F.B. Noronha, Appl. Catal., B 96 (2010) 387-398.

[45] O.A. Ferretti, G.J. Siri, F. Humblot, J.P. Candy, B. Didillon, J.M. Basset, React. Kinet. Catal. Lett. 63 (1998) 115-120.

[46] P. Chantaravitoon, S. Chavadej, J. Schwank, Chem. Eng. J. 97 (2004) 161-171.

[47] P. Chantaravitoon, S. Chavadej, J. Schwank, Chem. Eng. J. 98 (2004) 99-104.

[48] J.W. Bae, E.J. Jang, B.I. Lee, J.S. Lee, K.H. Lee, Ind. Eng. Chem. Res. 46 (2007) 1721-1730.

[49] A. Chongterdtoonskul, J.W. Schwank, S. Chavadej, J. Mol. Catal. A: Chem. 358 (2012) 58-66.

[50] A. Chongterdtoonskul, J.W. Schwank, S. Chavadej, Catal. Lett. 142 (2012) 991-1002.

[51] T. Puangpetch, S. Chavadej, T. Sreethawong, Energ. Convers. Manage. 52 (2011) 2256-2261.

[52] T. Puangpetch, P. Sommakettarin, S. Chavadej, T. Sreethawong, Int. J. Hydrogen Energy 35 (2010) 12428-12442.

[53] T. Puangpetch, T. Sreethawong, S. Yoshikawa, S. Chavadej, J. Mol. Catal. A: Chem. 287 (2008) 70-79.

[54] T. Puangpetch, T. Sreethawong, S. Yoshikawa, S. Chavadej, J. Mol. Catal. A: Chem. 312 (2009) 97-106.

[55] B.D. Cullity, Elements of X-ray Diffraction., Addison-Wesley Pub. Co., MA, 1978.

[56] A.G. Jackson, Handbook of Crystallography, Springer-Verlag, New York, 1991.

[57] J.F. Moulder, W.F. Stickle, P.E. Sobol, K.D. Bomben, Handbook of X Ray Photoelectron Spectroscopy: A Reference Book of Standard Spectra for Identification and Interpretation of XPS Data, Physical Electronics, 1995.

[58] S. Rojluechai, Ph.D. Dissertation, The Petroleum and Petrochemical College, Chulalongkorn University, Bangkok, Thailand, 2006.

[59] M.O. Ozbek, I. Onal, R.A. Santen, ChemCatChem. 3 (2011) 150-153.